

# Chromatographic Study of Surface Diffusion

PETR SCHNEIDER and J. M. SMITH

University of California, Davis, California

A new method, based upon chromatography, was used to measure surface diffusion coefficients for ethane, propane, and *n*-butane on silica gel. The diffusivities correspond to very low surface coverages (fraction of a monolayer of the order of  $10^{-4}$ ) and hence should represent limiting values. A survey of available surface diffusion information, all at higher coverages, indicated that the results reported here are at the lower end of the range of diffusivities. The activation energy and heat of adsorption, for example, for *n*-butane, were 4.4 and  $-7.8$  k cal./mole, respectively.

Surface diffusion was a significant fraction of the total intraparticle mass transport, in part because in the small pores in silica gel gas phase diffusion was solely by the Knudsen mechanism. For propane, surface migration was 73% of the total transport at  $50^{\circ}\text{C}$ . and 61.5% at  $125^{\circ}\text{C}$ .

In a previous paper (1) it was shown that all the rate constants necessary to describe the adsorption of a gas from an inert carrier stream could be evaluated by analysis of the chromatographic wave leaving the bed of porous particles. By using this method such constants, including intraparticle diffusivities, were determined for ethane, propane, and *n*-butane on silica gel.

The diffusivities so obtained indicated the presence of surface diffusion. Our purpose was to investigate experimentally the significance of surface migration, using the chromatographic method. The conditions were chosen so that equilibrium was obtained between the concentration of adsorbate in the gas phase in the pores and on the surface of the solid. This greatly simplifies the resolution of the measured total flux into surface and gas phase contributions. The gas phase diffusion in the pores of silica gel used here was solely of the Knudsen type, thus reducing its magnitude with respect to the surface contribution.

Both steady state and transient procedures have been published for evaluating surface diffusion. At steady state it is possible to establish the average surface concentration, or surface coverage, associated with the surface transport. However, it is not feasible to operate at very low surface coverages where the surface diffusivity should approach a constant value. With transient methods it is possible to operate in this region, but the surface coverage varies not only with position but also with time. The chromatographic method is a transient one, but the total pressure gradient, normally required for unsteady operation, is absent. It is easy to make measurements at very low concentrations on the solid surface. To our knowledge, surface diffusivities have not been measured heretofore at fractional coverages as low ( $10^{-4}$ ) as reported here.

## DESCRIPTION OF SURFACE DIFFUSION COEFFICIENTS

In order to analyze chromatographic curves when intraparticle surface diffusion is present, it is necessary to introduce a description of the surface transport into the set of differential equations representing the whole un-

steady state process. One possibility is to consider surface migration as a diffusional process in which the flux,  $N_s^*$ , expressed as the molal rate of flow per unit perimeter of pore surface perpendicular to the direction of flow, is given by the expression:

$$N_s^* = -D_s \frac{dc_s}{dx} \quad (1)$$

where the surface concentration of adsorbate  $c_s$  is defined as moles adsorbed per unit area of surface. The proportionality constant  $D_s$  is analogous to the diffusion coefficient in Fick's equation, and is, therefore, called surface diffusivity or surface diffusion coefficient. It has been shown experimentally (4 to 9), that the surface diffusion coefficient is not constant, but varies with surface concentration of the adsorbed substance. However, it appears (6) that for very low coverages (much less than a monolayer), this coefficient approaches a constant value. For example, Metzner and Weaver (10) when measuring the permeability of isobutane on Vycor glass have obtained nonzero permeability for very low pressures of isobutane. Also their theoretical treatment suggests that for surface coverages approaching zero the permeability coefficient tends to a finite value. It is therefore reasonable to use Equation (1) for describing surface transport provided the surface coverage is very low. It will be shown later that the chromatographic method permits measurements in the region where the coverage is of the order of fractions of a percent of a unimolecular layer.

The intraparticle mass balance of adsorbate, when diffusion occurs only by Knudsen flow in the gas phase of the pores, is normally written for a unit volume of the particle as follows:

$$\frac{D_K}{\beta} \left( \frac{\partial^2 c_i}{\partial r^2} + \frac{2}{r} \frac{\partial c_i}{\partial r} \right) = \frac{\partial c_i}{\partial t} + \frac{\rho_p}{\beta} \frac{\partial c_{ads}}{\partial t} \quad (2)$$

To include surface diffusion it is necessary to define a surface diffusion coefficient based on the surface flux through unit total area. Depending on the units of the surface concentration of adsorbate it is possible to write

$$N_s = -D_{s,p}(dc_{s,p}/dr) = -D_{s,ps}(dc_{s,ps}/dr) = -D_{s,s}(dc_{s,s}/dr) \quad (3)$$

Here the concentration is expressed as amount adsorbed per unit volume; namely, per unit volume of pore space

P. Schneider is on leave from the Institute of Chemical Process Fundamentals, Czechoslovak Academy of Sciences, Prague.

( $c_{s,p}$ ), or per unit of particle space ( $c_{s,ps}$ ), or per unit of the volume of the solid forming the particle ( $c_{s,s}$ ). All of these concentrations have been used by various authors to describe surface transport, and leads to confusion in comparing surface diffusivities from different sources. In terms of the concentration  $c_{s,p}$  the mass balance in a spherical particle of porous adsorbent, which takes into account transport in both the pore space and on the surface, can be expressed as

$$\frac{D_K}{\beta} \left( \frac{\partial^2 c_i}{\partial r^2} + \frac{2}{r} \frac{\partial c_i}{\partial r} \right) + \frac{D_{s,p}}{\beta} \left( \frac{\partial^2 c_{s,p}}{\partial r^2} + \frac{2}{r} \frac{\partial c_{s,p}}{\partial r} \right) = \frac{\partial c_i}{\partial t} + \frac{\partial c_{s,p}}{\partial t} \quad (4)$$

If the adsorption-desorption process is rapid with respect to diffusion, the gas and surface concentrations are in equilibrium: If this equilibrium can be described by a linear isotherm,  $K_A = c_{ads}/c_i$ , Equation (4) reduces to the form

$$\left( D_K + D_{s,p} \frac{\rho_p}{\beta} K_A \right) \left( \frac{\partial^2 c_i}{\partial r^2} + \frac{2}{r} \frac{\partial c_i}{\partial r} \right) = \beta \left( 1 + \frac{\rho_p}{\beta} K_A \right) \frac{\partial c_i}{\partial t} \quad (5)$$

since  $c_{s,p} = (\rho_p/\beta) K_A c_i$ . Under these restrictions Equation (2), in the absence of surface diffusion, becomes

$$D_K \left( \frac{\partial^2 c_i}{\partial r^2} + \frac{2}{r} \frac{\partial c_i}{\partial r} \right) = \beta \left( 1 + \frac{\rho_p}{\beta} K_A \right) \frac{\partial c_i}{\partial t} \quad (6)$$

If we define an overall diffusivity,  $D_c$ , as

$$D_c = D_K + (\rho_p/\beta) K_A D_{s,p} \quad (7)$$

Equations (5) and (6) are the same, except for the difference in meaning of  $D_c$ ; in Equations (6),  $D_c = D_K$ , and in Equation (5)  $D_c$  is given by Equation (7).

For other definitions of the concentration, and with the linear equilibrium restriction, there results

$$D_c - D_K = \frac{\rho_p}{\beta} K_A D_{s,p} = \rho_p K_A D_{s,ps} = \frac{\rho_p K_A}{1 - \beta} D_{s,s} \quad (8)$$

$$h(p) = \frac{3k_f}{R} \frac{1 - \alpha}{\alpha} \left[ \frac{1}{p} - \frac{\sinh(R\sqrt{\lambda})}{(p D_c/k_f)\sqrt{\lambda} \cosh(R\sqrt{\lambda}) + p \left( 1 - \frac{D_c}{k_f R} \right) \sinh(R\sqrt{\lambda})} \right] \quad (17)$$

To evaluate the relations between the true surface diffusion coefficient  $D_s$ , and effective coefficients  $D_{s,p}$ ,  $D_{s,ps}$ ,  $D_{s,s}$ , it is necessary to assume a model of the porous particle. If we adopt the simple model of parallel capillaries with a tortuosity factor  $q_{surf}$ , which is frequently used for discussions of gas diffusion, the relationships are as follows:

$$D_{s,p} = \frac{\beta}{q_{surf}} D_s; D_{s,ps} = \frac{1}{q_{surf}} D_s; D_{s,s} = \frac{1 - \beta}{q_{surf}} D_s \quad (9)$$

The effective gas diffusion coefficient,  $D_K$ , is then given as

$$D_K = \frac{\beta}{q_{int}} D_K \quad (10)$$

The tortuosity factors for surface and gas transport are not necessarily the same, hence they are identified by

different subscripts in Equations (9) and (10).

## METHOD OF EVALUATING DIFFUSIVITIES FROM CHROMATOGRAPHIC CURVES

The differential equations describing the concentration of adsorbate flowing under isothermal conditions with an inert carrier gas through a column filled with spherical adsorbent particles consists of a mass balance in the interparticle space

$$\frac{E_A}{\alpha} \frac{\partial^2 c}{\partial z^2} - v \frac{\partial c}{\partial z} - \frac{\partial c}{\partial t} - \frac{3Dc}{R} \frac{1 - \alpha}{\alpha} \frac{\partial c_i}{\partial r} \Big|_{r=R} = 0 \quad (11)$$

and a mass balance in the particle, Equation (5). The boundary conditions are

$$r = R, D_c \frac{\partial c_i}{\partial r} = k_f (c - c_i) \quad (12)$$

$$r = 0 \text{ and } t \geq 0, \frac{\partial c_i}{\partial r} = \frac{\partial c_{ads}}{\partial r} = 0 \quad (13)$$

The initial conditions describing the square wave input of adsorbate may be written

$$\begin{array}{lll} z = 0 & t = 0 & c = 0 \\ r \geq 0 & t = 0 & c_i = c_{ads} = 0 \\ z = 0 & 0 < t \leq t_{oA} & c = c_o \\ z = 0 & t > t_{oA} & c = 0 \end{array} \quad (14)$$

The Laplace-Carson transform of the concentration function  $c(z,t)$  is defined by

$$s(z,p) = p \int_0^\infty c(z,t) \exp(-pt) dt$$

By using this transformation Kubin (2,3) solved Equations (5), and (11) to (14), obtaining

$$s(z,p) = c_o [1 - \exp(-pt_{oA})] \exp(-\gamma z) \quad (15)$$

where

$$\gamma = -v/(2E_A/\alpha) + \sqrt{[v/(2E_A/\alpha)]^2 + [p/(E_A/\alpha)](1 + h(p))} \quad (16)$$

and

$$\lambda = p/(D_c/\beta) \quad (18)$$

The  $n$ th absolute ( $\mu'_n$ ) and central ( $\mu_n$ ) moments of the chromatographic curve are defined by Equations (19) to (21)

$$\mu'_n = m_n/m_o \quad (n = 0, 1, 2 \dots) \quad (19)$$

$$m_n = \int_0^\infty t^n c(z,t) dt \quad (n = 0, 1, 2 \dots) \quad (20)$$

$$\mu_n = (1/m_o) \int_0^\infty (t - \mu'_1)^n c(z,t) dt \quad (n = 0, 1, 2 \dots) \quad (21)$$

Since the following relation [Equation (22)] is valid for Laplace-Carson transforms:

$$m_n = \int_0^\infty t^n c(z,t) dt = (-1)^n \lim_{p \rightarrow 0} \frac{d^n}{dp^n} \left[ \frac{s(z,p)}{p} \right] \quad (22)$$

it is possible to evaluate explicitly the moments of the chromatographic curve. Thus the first absolute moment,  $\mu'_1$ , is

$$\mu'_1 = \frac{z}{v} (1 + \delta_o) + \frac{t_{oA}}{2} \quad (23)$$

The second and third central moments are

$$\mu_2 = \frac{2z}{v} \left[ \delta_1 + \frac{E_A}{\alpha} (1 + \delta_o)^2 (1/v^2) \right] + \frac{t_{oA}^2}{12} \quad (24)$$

$$\mu_3 = \frac{3z}{v} \left[ \delta_2 + \frac{4E_A}{\alpha} \delta_1 (1 + \delta_o) + 4 \left( \frac{E_A}{\alpha} \right)^2 (1 + \delta_o)^3 (1/v^4) \right] \quad (25)$$

where

$$\delta_o = \frac{1 - \alpha}{\alpha} \beta \left( 1 + \frac{\rho_p}{\beta} K_A \right) \quad (26)$$

$$\delta_1 = \frac{1 - \alpha}{\alpha} \frac{R^2 \beta^2}{15} \left( 1 + \frac{\rho_p}{\beta} K_A \right)^2 \left( \frac{1}{D_c} + \frac{5}{k_f R} \right) \quad (27)$$

$$\delta_2 = \lim_{p \rightarrow 0} \frac{d^2}{dp^2} [h(p)] \quad (28)$$

In the preceding paper (1) it was demonstrated, that at low Reynolds number the external mass transfer coefficient did not depend on the carrier gas velocity. It was shown therefore that  $k_f$  could be calculated from the relation  $N_{NuAB} = 2.0$ , where the Sherwood number is  $N_{NuAB} = 2R k_f / \mathcal{D}_{AB}$ . By using the resulting relation  $k_f R = \mathcal{D}_{AB}$  in Equation (27) the effective diffusion coefficients,  $D_c$ , can be calculated from the experimental second central moments,  $\mu_2$ , for a series of chromatographic curves measured for different carrier gas velocities,  $v$ . The necessary adsorption coefficients,  $K_A$ , can be obtained by means of Equation (23) from the experimental first absolute moments,  $\mu'_1$ , using the same series of chromatographic curves. Finally Equation (7) can be used to evaluate the surface diffusivity from  $D_c$ . To do this requires a knowledge of the effective Knudsen diffusion coefficient  $D_K$ . This is usually obtained by measurements with a non-adsorbable gas. However, the flame ionization detector, which was used in this study, because of its high sensitivity, does not respond to inert gases like helium. Therefore an adsorbable gas was used for this purpose, but at high temperatures. In any event the true Knudsen diffusivity must be known. This was calculated from

$$D_K = (4/3) \bar{r} \sqrt{2R_g T / (\pi M)} \quad (29)$$

Equation (29) is satisfactory when the mean free path of the adsorbate molecules is large in comparison with the pore diameter. In the experimental work reported here the pressure was atmospheric and the mean pore radius of the silica gel adsorbent was 11 Å. Under these conditions Equation (29) is justified.

## SCOPE OF EXPERIMENTS

Chromatographic curves were measured for propane at 50, 75, 100 and 125°C., for *n*-butane at 50, 100, 125, and 150°C., and for ethane at 50, 175, and 200°C. The particle size of silica gel was  $R = 0.50$  mm. It was shown earlier (1) that for this particle size and at 50°C. the resistance of the surface process of adsorption was negligible in comparison with the intraparticle mass transport resistance. Hence at 50°C. and higher temperatures, the adsorption equilibrium assumption employed in Equation

(5) is justified.

Carrier gas velocities varied from  $v = 1.5 - 15$  cm/sec. In the relatively short chromatographic column ( $z = 13.0$  cm.) the difference between the inlet and outlet total pressures was but several millimeters of mercury, in the worst case. Hence, it was possible to assume constant pressure, in agreement with the implicit assumption upon which the chromatographic theory is based.

The adsorbate gas was injected as a square function of concentration in accordance with Equation (14). To determine the dispersion of the square wave between sample injection and entrance to the bed of particles, moments were measured when the bed of particles was removed and the detector placed where the bed had been. For *n*-butane at 50°C., with a carrier gas flow rate of 49.6 cc./min., the first and second moments were 0.1 sec. and 0.015 sq. sec., respectively. These values are negligible with respect to about 10 sec. and 30 sq. sec., measured in the effluent from the bed. Hence, the assumption of a square wave input to the bed is valid. Instead of injecting pure hydrocarbons in the stream of helium, mixtures of hydrocarbon with helium were injected into the carrier gas. The concentration of hydrocarbon in this mixture was 0.9-1.0 vol. % for ethane and propane and 0.5 vol. % for *n*-butane. At these low concentrations the adsorption isotherm is linear as required in Equation (5). Evidence for this was obtained (1) in the same system by direct measurement of the isotherms, and by comparison of equilibrium constants,  $K_A$ , obtained from chromatography [Equation (23)] with those evaluated directly.

## EXPERIMENTAL PROCEDURE

### Adsorbent

Silica gel was fractured and ground, and the fraction with  $R = 0.50 \pm 0.03$  mm. separated by sieves. The diameter of the equivalent spherical particle was taken as the average of the sieve openings. The gel was pretreated in place in the column by heating in a stream of helium at 200°C. for 18 hr. Masamune and Smith (11) used the same gel and reported the following properties: specific surface area 832 sq.m./g., void volume 0.43 ml./g., internal void fraction  $\beta = 0.486$ , particle density  $\rho_p = 1.13$  g./ml. The average pore radius, calculated as  $2(\text{void vol.})/(\text{surface area})$ , is  $r = 11$  Å.

### Gases

The helium had a stated purity of better than 99.99%. It was dried by passing through a metal trap cooled in an acetone-dry ice bath. The helium-hydrocarbon streams were prepared as elsewhere (1) by mixing streams of synthetic helium-hydrocarbon mixtures and pure helium. These streams were dried in an acetone-dry ice trap and then retained in sample loops of different volumes. To make a run, the gas mixture in the loop was flushed into the column with carrier gas (pure helium).

### Chromatograph

A constant temperature, gas chromatograph (Model 600-D, Varian Aerograph) with a flame ionization detector was used. A detailed description of this apparatus and of the six-way, two-position sampling valve used for injection of the square function of concentration is given elsewhere (1). The column ( $z = 13.0$  cm.) was of  $\frac{3}{8}$  in. O.D. copper tubing; cross-sectional area 0.472 sq. cm. The external void fraction of the column packed with silica gel was  $\alpha = 0.340$ . The intraparticle void volume per unit of interparticle voids,  $\beta(1 - \alpha)/\alpha = 0.945$ .

## EVALUATION OF MOMENTS OF THE CHROMATOGRAPHIC CURVES

The moments,  $\mu'_1$  and  $\mu_2$ , were evaluated according to Equations (30) to (32)

$$\mu'_1 = m'_1 / m'_o \quad (30)$$

$$\mu_2 = \mu'_2 - (\mu'_1)^2 \quad (31)$$

where

$$\mu'_2 = m'_2/m'_0 \quad (32)$$

and  $m'_1$  and  $m'_2$  have the same meaning as  $m_1$  and  $m_2$  in Equation (20), except that the outlet concentration,  $c(z,t)$ , is replaced by the deflection  $w(t)$  of the recorder pen connected with the ionization detector at the column outlet. Thus

$$m'_n = \int_0^\infty t^n w(t) dt, \quad (n = 0, 1, 2, \dots)$$

This transformation is valid because of the direct proportionality between the recorder pen deflection and the concentration in the detector. The integrals  $m'_0$ ,  $m'_1$ , and  $m'_2$  were evaluated numerically from the experimental chromatographic curves using Simpson's rule on an IBM 7044 computer.

## RESULTS AND DISCUSSION

### EQUILIBRIUM ADSORPTION CHARACTERISTICS FROM THE FIRST ABSOLUTE MOMENT

For an inert or nonadsorbable gas ( $K_A = 0$ ), Equations (23) and (26) show that the first absolute moment is

$$(\mu'_1)_{\text{inert}} = [1 + \beta(1 - \alpha)/\alpha](z/v) \quad (33)$$

when the injection time  $(t_0)_{\text{inert}} = 0$ . Then the reduced first moment is given by

$$[\Delta\mu'_1 - (t_{0A}/2)]/[\beta(1 - \alpha)/\alpha] = (\rho_p/\beta)K_A(z/v) \quad (34)$$

where

$$\Delta\mu'_1 = \mu'_1 - (\mu'_1)_{\text{inert}}$$

This equation shows that the adsorption equilibrium constant,  $K_A$ , can be evaluated from the slope of the linear plot of  $[\Delta\mu'_1 - (t_{0A}/2)]/[\beta(1 - \alpha)/\alpha]$  vs.  $z/v$ . As an illustration, the experimental results for propane are so plotted for different temperatures in Figure 1. The experimental points for particle sizes  $R = 0.11$  and  $0.39$  mm. were taken from (1). The temperature dependence of  $K_A$  obtained from such plots for all three hydrocarbons are

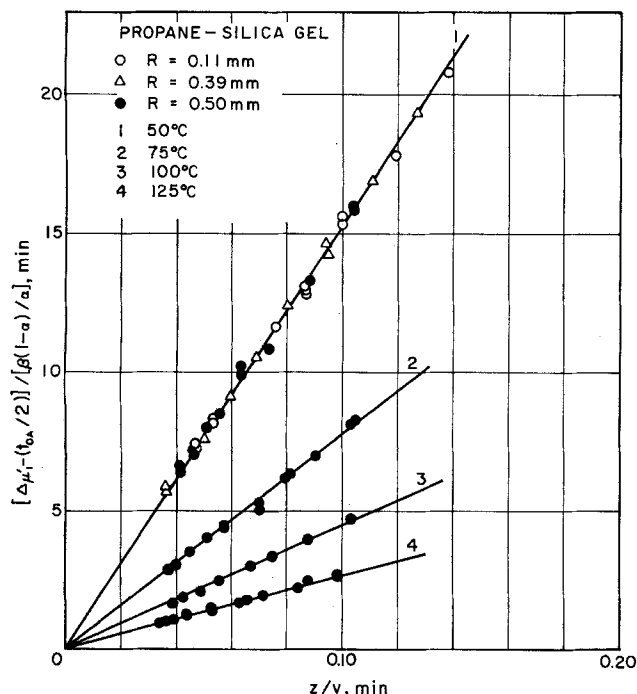


Fig. 1. Correlation of reduced first moment for propane.

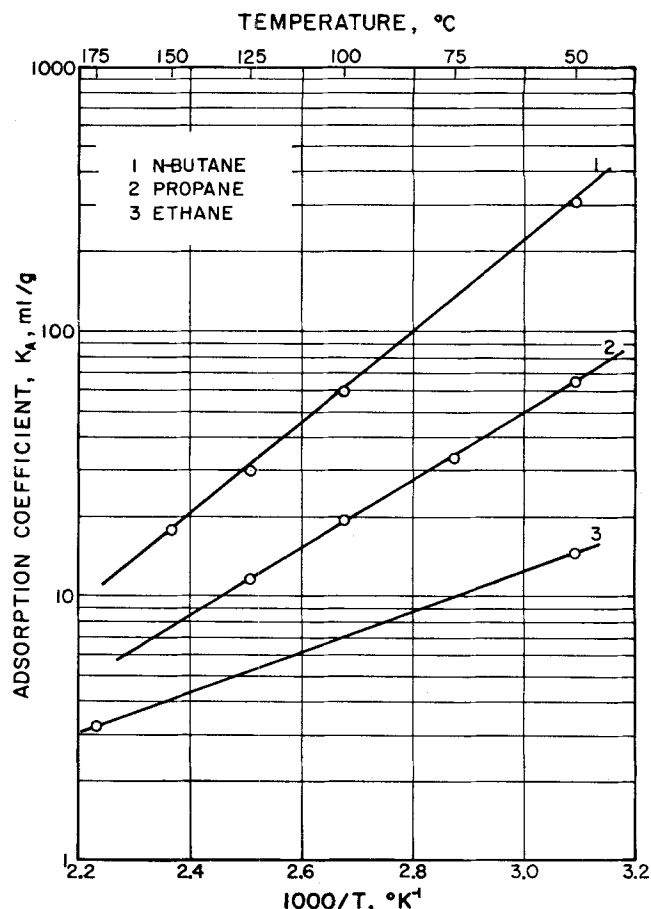


Fig. 2. Temperature dependence of adsorption equilibrium constants.

summarized in Figure 2. It is worth noting that Eberly and Spencer (12) found from chromatography that the adsorption coefficient of *n*-butane on silica gel at 60°C. was 225 ml./g. From line 1 in Figure 2, essentially the same result is obtained.

Heats of adsorption,  $\Delta H_{\text{ads}}$ , calculated from the van't Hoff equation using the slopes of the lines in Figure 2 were  $-3.5$ ,  $-5.9$ , and  $-7.8$  kcal./g.mole for ethane, propane, and *n*-butane, respectively. These results are each higher than the heats of condensation of the hydrocarbons at their normal boiling points, although the comparison is not very meaningful because of the difference in temperature between condensation and adsorption.

Haul's (14) measurement of the adsorption heat of *n*-butane on Linde Silica, extrapolated to zero coverage, is  $-7.5$  kcal./mole. This compares well with 7.8 kcal./mole found in this study. Surprisingly, the adsorption heat of isobutane on Vycor glass, given in the literature (10) as  $-7.1$  kcal./mole, is also close to the value for *n*-butane on silica gel. The adsorption heats of propane and ethane on industrial silica alumina cracking catalyst, found by Barrer and Gabor (15) to be  $-5.7$  and  $-4.1$  kcal./mole, respectively, are in reasonable agreement with the values found here.

### AXIAL DISPERSION AND INTRAPARTICLE DIFFUSION CONSTANTS FROM THE SECOND CENTRAL MOMENT

For correlation purposes it is advantageous to rewrite Equations (24) and (27) in a modified form:

$$[\mu_2 - (t_{0A}^2/12)]/(2z/v) = \delta_e + \delta_i + (E_A/\alpha)(1 + \delta_o)^2(1/v^2) \quad (35)$$

where

$$\delta_e = \delta_o(R^2\beta/15) \left( 1 + \frac{\rho_p}{\beta} K_A \right) (1/D_c) \quad (36)$$

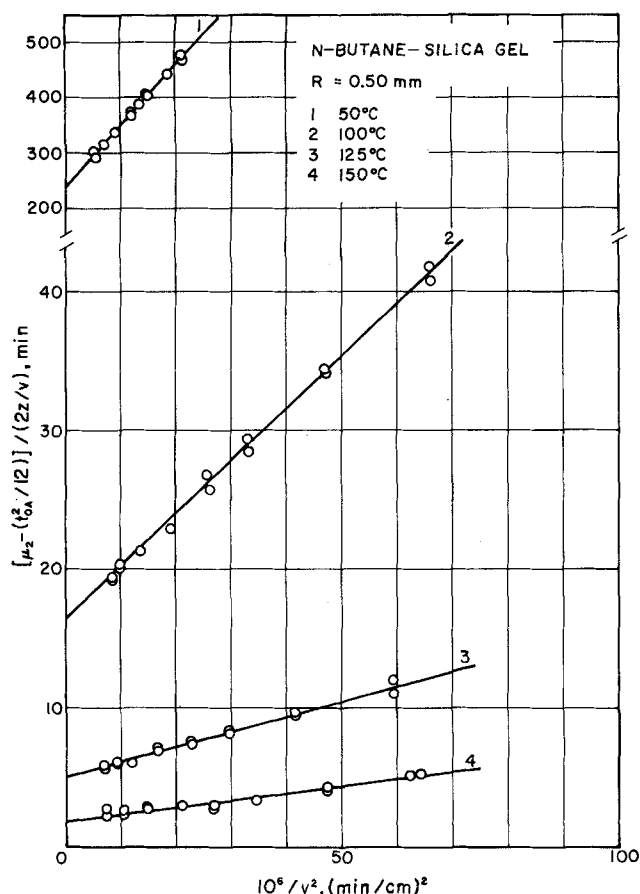


Fig. 3. Correlation of second central moment for *n*-butane.

$$\delta_i = \delta_o(R^2\beta/15) \left( 1 + \frac{\rho_p}{\beta} K_A \right) (5/k_f R) \quad (37)$$

and  $\delta_o$  is given by Equation (26).

According to Equation (36)  $\delta_i$  does not depend on the gas velocity,  $v$ . Also if  $\delta_o$  is velocity independent, a plot of  $[\mu_2 - (t^2_{oA}/12)] / (2z/v)$  vs.  $(1/v^2)$  should result in a straight line. The experimental data were plotted in this manner and are illustrated in Figure 3 for butane. The data points fulfill the straight line dependence, a result that was also obtained in reference 1. By using the relationship  $k_f R = \mathcal{D}_{AB}$ , mentioned previously, it can be shown that  $\delta_o$ , characterizing the external mass transfer contribution to the second central moment, is at least two orders of magnitude less than the  $\delta_i$ , characterizing intraparticle transport. Thus the influence of the external mass transfer is very small in comparison with the intraparticle transport processes.

The adsorption coefficient,  $K_A$  and hence  $\delta_o$ , is known from the analysis of the first absolute moments, and the external mass transfer coefficient,  $k_f$ , can be estimated from the above relationship. Therefore, it is possible to evaluate the axial dispersion coefficient,  $E_A$ , and the effective diffusion coefficients,  $D_e$ , from the slopes and intercepts of the straight lines using Equations (35) to (37) and (26).

The values of  $E_A$  so established are summarized in Table 1, together with the external tortuosity factors,  $q_{ext}$ , defined by

$$E_A = (\alpha/q_{ext}) \mathcal{D}_{AB} \quad (38)$$

This equation is based upon a model of the packed bed of adsorbent frequently used for porous media; that is, smooth, cylindrical capillaries with the same average diameter, running in the direction of the gas flow. The

tortuosity factor then expresses the average length of the pass of the flowing gas relative to the shortest possible pass. It is also supposed that the axial dispersion is due only to molecular diffusion in the interparticle space. According to this model,  $q_{ext}$  should not depend on the kind of the gas or on the temperature. From the data in Table 1 it is seen that  $q_{ext}$  follows this pattern. The variation of  $q_{ext}$  for a particular hydrocarbon shows no trend with temperature, nor is there any influence of hydrocarbon structure. To illustrate the results, Figure 4 shows the experimental  $E_A$  values for propane together with the coefficients predicted from Equation (38) with specific tortuosities. Also the upper line in the figure gives the molecular diffusivity in the propane-helium system.

TABLE 1. AXIAL DISPERSION COEFFICIENTS,  $E_A$ , AND TORTUOSITY FACTORS,  $q_{ext}$ , FOR SILICA GEL PARTICLES WITH  $R = 0.50$  mm. ( $\alpha = 0.34$ )

Temperature °C.	Ethane	$E_A$ , sq.cm./sec.; $q_{ext}$ Propane	$n$ -Butane
50	0.130; 1.55	0.125; 1.31	0.130; 1.21
75	—	0.146; 1.28	—
100	—	0.158; 1.32	0.119; 1.69
125	—	0.174; 1.34	0.137; 1.65
150	—	—	0.170; 1.46
175	0.232; 1.50	—	—
200	0.237; 1.50	—	—
Average $q_{ext}$	1.52	1.31	1.50

1. The molecular diffusivities,  $\mathcal{D}_{AB}$ , were calculated from Hirschfelder's equation (16) using potential energy constants  $\epsilon/k$  and  $\sigma$  for ethane and propane given by Bird, Stewart, and Lightfoot (16). Potential energy constants for *n*-butane were taken from Reid and Sherwood (17).

2. Average  $q_{ext}$  for all hydrocarbons and all temperatures is 1.43.

The effective intraparticle diffusion coefficient,  $D_e$ , obtained from the intercepts of Figure 3 are summarized in Figure 5. The Knudsen diffusivities calculated from Equation (29) also are shown. Whereas the Knudsen diffusivity increases slightly with temperature,  $D_e$  decreases with temperature increase. This is expected when surface transport is significant. Thus  $(\rho_p/\beta) K_A D_{s,p}$  in Equation (7) will decrease with temperature as long as the activation energy,  $E_s$ , for surface diffusion is less in absolute magnitude than the heat of adsorption.  $E_s$  will always be less than  $|\Delta H_{ads}|$  according to the concept that surface migration occurs by movement of partially desorbed molecules along the surface.

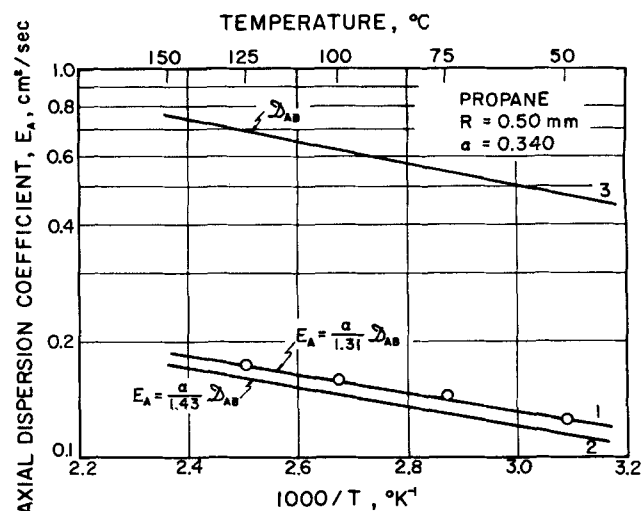


Fig. 4. Temperature dependence of  $E_A$  for propane (0, experimental points; 1, calculated with  $q_{ext} = 1.31$ ; 2, calculated with  $q_{ext} = 1.43$ ; 3, calculated molecular diffusivities  $\mathcal{D}_{AB}$ ).

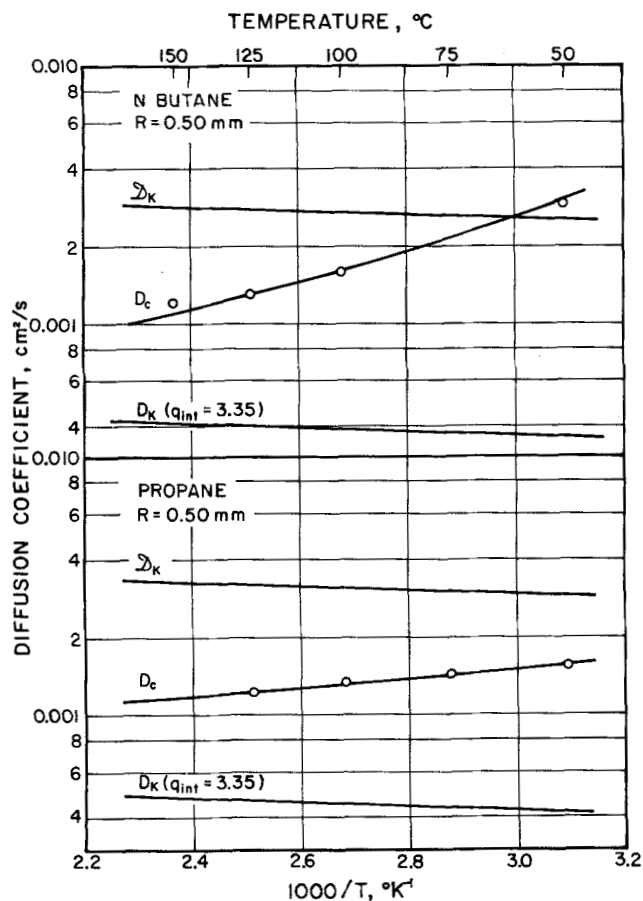


Fig. 5. Temperature dependence of the intraparticle diffusion coefficient,  $D_c$  (O, experimental points; lines for  $D_c$  calculated by means of Equation (7), using adsorption coefficients from Figure 2,  $D_{s,p}$  from Figure 8, and  $q_{int} = 3.35$ ).

#### SURFACE COVERAGE

The surface diffusivity normally depends upon the fraction of the surface covered by adsorbed molecules. In our experiments the surface coverage varies with time and position in the bed. This variation can be predicted approximately from the equations of Kubin (2) and Kucera (18) using the values of the constants  $K_A$ ,  $E_A$ ,  $D_c$  and  $k_f$  already established. According to these authors the concentration of the adsorbable gas in the interparticle space,  $c(z, t)$ , can be expressed by means of a series expansion using Hermitian polynomials:

$$c(z, \tau) = c_0 t_0 \exp(-\tau^2) \sum_{n=0}^{\infty} a_n H_n(\tau) \quad (39)$$

where

$$H_n(\tau) = (-1)^n \exp(\tau^2) \frac{d^n}{d\tau^n} [\exp(-\tau^2)] \quad (40)$$

and

$$\tau = (t - \mu'_1) / \sqrt{2\mu_2} \quad (41)$$

The coefficients,  $a_n$ , can be expressed (2) in terms of the moments of the chromatographic curve. The equation up to  $a_4$  are

$$a_0 = \frac{1}{\sqrt{2\pi\mu_2}} \quad (42)$$

$$a_1 = a_2 = 0 \quad (43)$$

$$a_3 = \frac{1}{2^2(3!)\sqrt{\pi}} \left( \frac{\mu_3}{\mu_2^2} \right) \quad (44)$$

$$a_4 = \frac{1}{2^{5/2}(4!)\sqrt{\pi\mu_2}} \left( \frac{\mu_4}{\mu_2^2} - 3 \right) \quad (45)$$

The central moments  $\mu_2$  and  $\mu_3$  are given by Equations (24) and (25); expressions for  $\mu_4$  and higher moments can be obtained from Equations (21) and (22).

From Equation (39) the concentration of adsorbable gas in the interparticle space can be evaluated as a function of bed length for  $\tau = 0$ ; that is, the concentration corresponding to the maximum (more exactly to the time of the center of gravity) of the chromatographic wave. Results for propane at typical conditions are shown by the curve in Figure 6. For the computations, the series expansion was terminated after the  $a_4$  term. The maximum gas concentration of the wave leaving the bed is known from experimental measurements. This value is also noted on the figure.

The curve in Figure 6 shows that the interparticle concentration decreases very rapidly as the wave travels through the bed. Since the curve represents the maximum concentration, the average value for the wave will be much lower. Furthermore, the large intraparticle diffusion resistance means that the concentration within the particle will be even less. Thus the results in Figure 6 depict the upper limit of possible gas concentrations. The ordinate at the right side gives the fractional surface coverage (fraction of a monolayer) as evaluated by assuming the surface to be in equilibrium with the interparticle gas concentration. For the calculations, the area occupied by one adsorbed propane molecule was taken as  $30.3 \text{ \AA}^2$  as suggested by Taylor and Atkins (19). From these results the average surface coverage during the chromatographic process is of the order of  $\theta_{\text{propane}} = 10^{-4}$ , or less.

Additional evidence of the low concentrations involved is given in Figure 7 where experimentally determined maximum concentrations of the peak at the column outlet are shown for butane for different velocities of carrier

#### MAX. CONC. OF THE CHROMATOGRAPHIC PEAK, $c/c_0$ , %

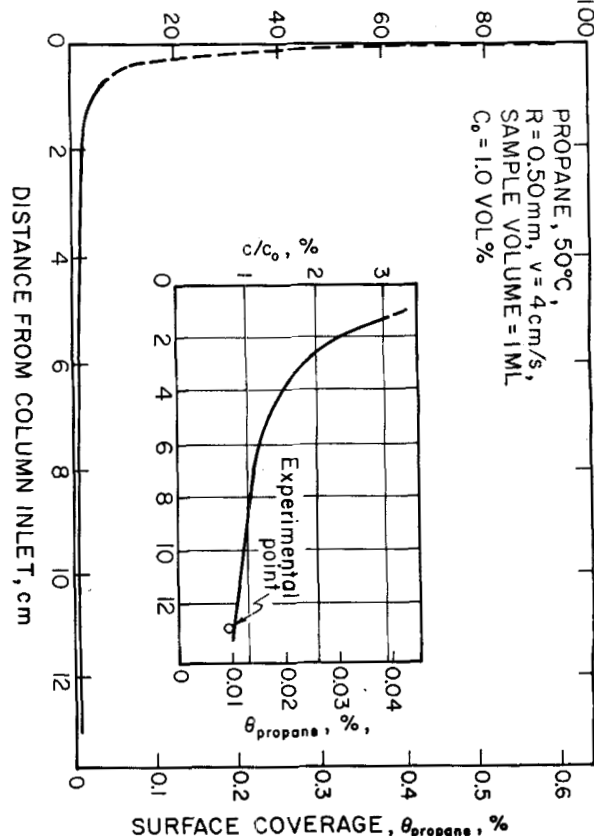


Fig. 6. Variation in maximum concentration of the chromatographic peak along the column.

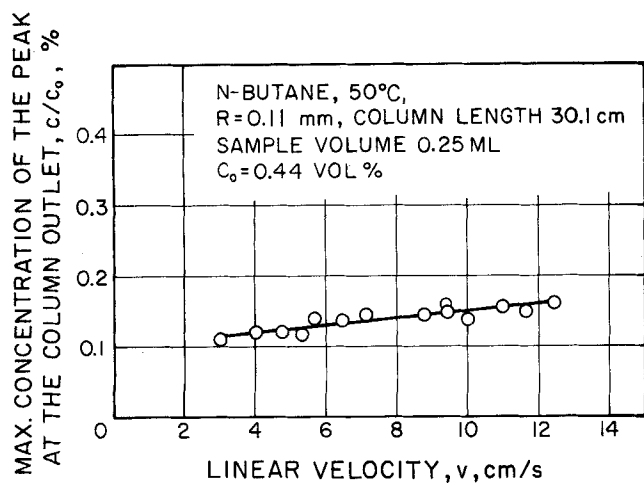


Fig. 7. Influence of carrier gas velocity on the maximum concentration of the chromatographic peak at the column outlet.

gas. Again the maximum outlet concentrations are of the order of  $10^{-2}$  vol. %. The surface coverage of the adsorbent here is then of a similar order as that for propane.

The very low average surface coverages are a special feature of this method of studying surface diffusion. It seems probable that under such conditions the surface diffusion coefficient will be approximately constant. Usually experimental methods for measurement of surface diffusivities operate where the surface coverage is about a complete monolayer or higher. The lowest coverages were of the order of one-tenth of a monolayer (8). In this respect the paper of Goring and deRosset (20) is an exception. These authors have used a somewhat similar experimental technique, nonsteady elution of the adsorbed substance from the adsorbent, so that the average coverages lie between the values commonly used and those of this study.

## SURFACE DIFFUSIVITIES

To separate the surface diffusivity from the experimentally determined  $D_c$  by using Equation (7), the effective Knudsen diffusion coefficient  $D_K$ , or the intraparticle tortuosity factor must be known. As already noted,  $D_K$  could not be measured directly. Another approach, described in the following paragraph, was adopted.

With increasing temperature  $D_K$  in Equation (7) increases slightly, while the term  $(\rho_p/\beta)K_A D_{s,p}$  decreases, due to the dominating influence of temperature on  $K_A$ . Therefore it is possible to measure  $D_c$  at so high a temperature that  $(\rho_p/\beta)K_A D_{s,p}$  will be negligible, and  $D_K = D_c$ . Then the intraparticle tortuosity factor  $q_{int}$ , according to Equation (10), becomes equal to  $\beta D_K/D_c$ . This value for  $q_{int}$  can then be used in Equation (10) to establish  $D_K$  at other temperatures. These values of  $D_K$  along with  $D_c$  may be employed in Equation (7) to determine  $D_{s,p}$ . This method will be better the lower the absorptivity of the adsorbate chosen for the high temperature measurement. Hence ethane was chosen, and chro-

matographic experiments made at several temperatures. Analysis of the data according to Equations (35) to (37) showed that  $\beta D_K/D_c = 1.2$  at  $50^\circ\text{C}$ ., 3.34 at  $175^\circ\text{C}$ ., and 3.35 at  $200^\circ\text{C}$ .. Since  $\beta D_K/D_c$  did not increase appreciably above  $175^\circ\text{C}$ ., it was assumed that  $D_c = D_K$  at  $200^\circ\text{C}$ ., and that  $q_{int} = 3.35$ . The values of  $D_K$  calculated from this tortuosity factor are shown as a function of temperature in Figure 5. The difference between curves for  $D_c$  and  $D_K$  on this figure is, according to Equation (7), equal to  $(\rho_p/\beta)K_A D_{s,p}$ .

Weisz and Schwartz (21) proposed, on the basis of their spherical cell model of porous structure, the expression

$$q_{int} = \sqrt{3}/1.5\beta$$

which yields, for the silica gel used here,  $q_{int} = 2.38$ . From the experimental results which these authors present there follows another possible expression, that is  $q_{int} = 2\sqrt{2} = 2.83$ . Both of these values as well as those summarized by Satterfield and Sherwood (22) are similar in magnitude to  $q_{int} = 3.35$  obtained from this study.

The effective surface diffusivities, calculated from the experimental  $D_c$  results, and using this value of  $q_{int}$ , are plotted in Figure 8 as a function of temperature. To illustrate relative numerical values,  $D_c$ ,  $D_K$  and  $(\rho_p/\beta)K_A D_{s,p}$  are given in Table 2 for propane. The activation energies for surface diffusion, calculated from the relation,  $D_{s,p} = (\text{const}) \exp(-E_s/R_g T)$ , are similar for propane and *n*-butane (propane,  $E_s = 4.5$  kcal./mole; *n*-butane,  $E_s = 4.4$  kcal./mole) and are equal to 76 and 56% of the heats of adsorption of propane and *n*-butane, respectively.

The importance of surface diffusion relative to the total intraparticle transport can be visualized by means of the ratio  $(\rho_p/\beta)K_A D_{s,p}/D_c$ . At  $50^\circ\text{C}$ ., surface diffusion forms 64, 73 and 87.5% of the total transport for ethane, pro-

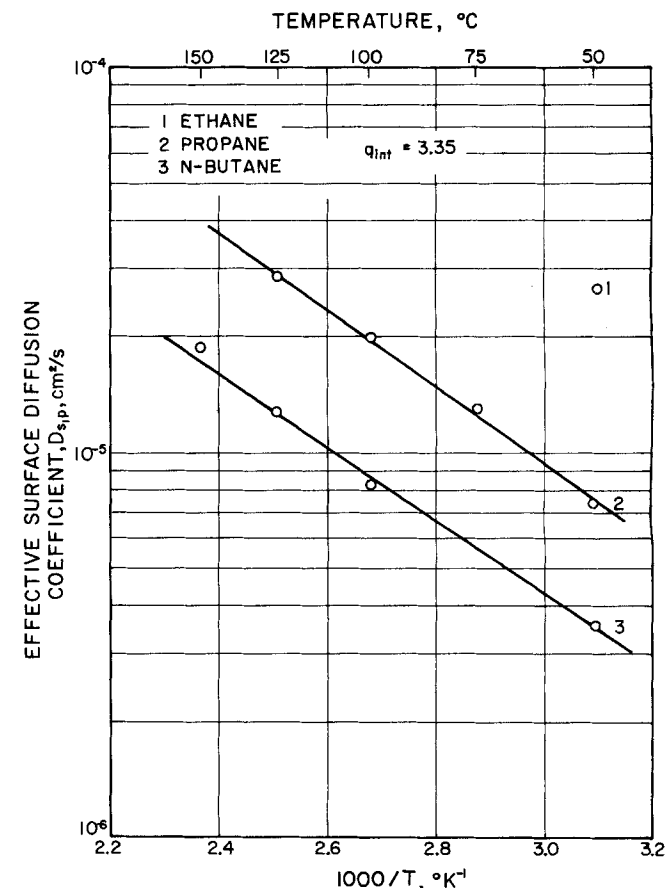


Fig. 8. Effective surface diffusion coefficients,  $D_{s,p}$ .

TABLE 2. DIFFUSION OF PROPANE

Temperature (°C.)	$D_c 10^3$ sq.cm./sec.	$D_K 10^3$ sq.cm./sec.	$(\rho_p/\beta)K_A D_{s,p} 10^3$ sq.cm./sec.	$D_{s,p} 10^5$ sq.cm./sec.
50	1.54	0.42	1.12	0.74
75	1.45	0.44	1.01	1.31
100	1.33	0.45	0.88	1.95
125	1.22	0.47	0.75	2.80

TABLE 3. SURFACE DIFFUSIVITIES OF ETHANE, PROPANE AND BUTANE

Adsorbent	Surface area sq.m./g.	Intraparticle void fraction, $\beta$ , %	Average pore radius $\bar{r}$ , Å	Temperature °C.	$D_{s,ps}$ sq.cm./sec.	Approximate surface coverage (% of monolayer	Activation energy, $E_s$ , kcal./ mole	$E_s/\Delta H_{ads}$ %	Method of measure- ment	Ref.
ETHANE										
Alumina	158	69	43	22	$2.4 \times 10^{-4}$	0 to 5			*	(20)
Silica alumina (96% SiO <sub>2</sub> )	600	46	15	22	$4.3 \times 10^{-5}$	0 to 5			*	(20)
Silica alumina cracking catalyst	360	40	17	50	$1.4 \times 10^{-4}$	†			††	(15)
				137	$3.9 \times 10^{-4}$	†	2.9	70	†	(15)
				50	$6.5 \times 10^{-5}$	†			††	(15)
				137	$1.9 \times 10^{-4}$	†	3.4	82	§	(15)
		53	25	50	$3.9 \times 10^{-4}$	†			††	(15)
				137	$17.5 \times 10^{-4}$	†	3.3	80	†	(15)
				50	$2.0 \times 10^{-4}$	†			††	(15)
				137	$5.4 \times 10^{-4}$	†	4.2	100	§	(15)
Silica gel	832	49	11	50	$5.5 \times 10^{-5}$	<<1				this paper
Vycor glass	140	30	30	50	$7.0 \times 10^{-5}$	†			†, §	(23)
				70	$9.0 \times 10^{-5}$	†	3.2	68	†, §	(23)
PROPANE										
Alumina	200		45	50	$1.1 \times 10^{-5}$ to $12 \times 10^{-5}$	3 to 35			†	(24)
Alumina	158	69	43	22	$4.8 \times 10^{-5}$	0 to 15			*	(20)
Silica alumina	360	40	17	180	$2.5 \times 10^{-4}$	†			†	(15)
cracking catalyst				180	$1.5 \times 10^{-4}$	†			§	(15)
		53	25	50	$2.1 \times 10^{-4}$	†			††	(15)
				137	$6.5 \times 10^{-4}$	†	3.3	59	†	(15)
				50	$5.6 \times 10^{-5}$	†			††	(15)
				137	$3.1 \times 10^{-4}$	†	5.0	90	§	(15)
Silica gel	832	49	11	50	$1.5 \times 10^{-5}$	<<1	4.5	76		this paper
Silica alumina (96% SiO <sub>2</sub> )	600	46	15	22	$3.3 \times 10^{-5}$	0 to 20			*	(20)
N-BUTANE										
Spheron 6 (2,700°) carbon black	84	54	140	30	$1.6 \times 10^{-5}$	25			†	(9)
				50	$2.3 \times 10^{-5}$	25	4.5	56	††	(9)
Pt-Alumina	164	62	54	21	$1.4 \times 10^{-5}$	20-30			†	(25)
Alumina	200		45	25	$3.6 \times 10^{-6}$	20 to 90			†	(24)
					to $9.7 \times 10^{-6}$				#	
Linde silica	300	72	80	-14	$9.3 \times 10^{-5}$	95			**	(14)
				50	$4.3 \times 10^{-4}$	95	4.0	66	††	(14)
		53		-14	$5.4 \times 10^{-5}$	95			**	(14)
				50	$1.6 \times 10^{-4}$	95	2.9	48	††	(14)
Linde silica	300	52		-10	$1.5 \times 10^{-5}$	10			†	(7)
		72		-10	$3.0 \times 10^{-5}$	10			†	(7)
Silica gel	832	49	11	50	$7.3 \times 10^{-6}$	<<1	4.4	56		this paper
ISOBUTANE										
Alumina	158	69	43	22	$4.7 \times 10^{-5}$	0 to 30			*	(20)
Silica alumina (96% SiO <sub>2</sub> )	600	46	15	22	$1.9 \times 10^{-5}$	0 to 50			*	(20)
Vycor glass	140	31	31	0	$3.0 \times 10^{-5}$	15			†	(5)
				50	$7.1 \times 10^{-5}$	15	3.0	40-50	††	(5)
Vycor glass		28	20	25	$4.4 \times 10^{-5}$ to $7.2 \times 10^{-5}$	3 to 80			†	(10)

\* Transient elution of adsorbed substance.

† In the range of validity of the linear isotherm.

‡ Permeability measurement under steady state.

§ Unsteady state flow [time lag method of Barrer (26)].

|| Evaluation of the moments of chromatographic curves.

#  $D_{s,p}$ .

\*\* Evaluation of adsorption kinetics.

†† Extrapolated.



pane and *n*-butane. At 125°C, 61.5% of propane is still transported by the surface process. At the same temperature the surface transport of *n*-butane represents 68.5% of the total.

Table 3 summarizes some of the results of studies of surface diffusion of ethane, propane, and butanes, given in the literature. Only those papers were included which were concerned with surface transport at coverages less than a monomolecular layer. The diffusivities are expressed as  $D_{s,ps}$ , which according to the Equation (9), is closely related to the true surface diffusion coefficient,  $D_s$ . The data in the table were obtained in many cases by recalculation of the original results; for example when the permeability concept (surface flow) was used rather than diffusion. When the original data were insufficient for such recalculation, estimates were made. In order to obtain diffusion coefficients at 50°C., for comparison with the results of this study, it was sometimes necessary to extrapolate the literature data beyond the temperature interval in which they were obtained. In many cases the degree of coverage was not explicitly stated; the values presented in Table 2 are, therefore, only approximate estimates, based usually on the original sorption data.

It is noted that the surface diffusion coefficients are usually of the order  $10^{-4}$  to  $10^{-5}$ . Also activation energies,  $E_s$ , lie usually between 3 and 5 kcal./mole. This is rather striking in view of the wide spectrum of the adsorbents [from nonpolar Spheron 6 (2,700°) carbon black to polar aluminosilicate catalysts]. Though the influence of the chemical character of the adsorbent surface is in some degree camouflaged by the simultaneously changing texture (physical structure) of the sorbents, it seems that the role of the chemical nature of the adsorbent is not strong for the systems listed in the table. Apparently, a more significant variable is the texture of the adsorbent. If this is so, surface transport resembles in many aspects gaseous diffusion in porous solids where also the chemical nature of the solid is not important but texture is.

The data in Table 3 show that the activation energies for propane and *n*-butane from this study lie rather close to the values of other authors. On the other hand, diffusivities from this work are at the lower limit of the tabulated results. This is not surprising because of the very low surface coverages in our work. Though the average surface coverages are orders of magnitude lower than those of other studies, the differences between the surface diffusion coefficients are not so marked. This indicates that diffusivities obtained at coverages of about one-tenth of a monolayer are not far from the values on a nearly bare surface.

Some sets of data in Table 3 make it possible to compare diffusion coefficients for different hydrocarbons on the same adsorbent: for example, Gorring and deRosset's (20) data for alumina and silica alumina (96% silica) and the data for silica-alumina industrial cracking catalyst of Barrer and Gabor (15). Though the comparison is not very conclusive, the surface diffusion coefficients appear to decrease with increasing molecular weight of the hydrocarbon. This conclusion is supported by our results which show that  $D_{s,p}$ , very roughly, is inversely proportional to the square root of the molecular weight of the hydrocarbon.

## CONCLUSIONS

By analyzing the moments of chromatographic curves, it is possible to evaluate intraparticle effective diffusion coefficients, from which surface diffusivities can be extracted. An advantage of this method is that the average surface coverage is very low. Thus the surface

diffusion coefficients so obtained are very close to limiting values. The activation energy for surface diffusivities of propane and *n*-butane were found to be 4 to 5 kcal./mole in agreement with values reported by others. The diffusivities decrease with increasing molecular weight of the hydrocarbon adsorbed on the silica gel.

## ACKNOWLEDGMENT

The financial assistance provided for this study by the Petroleum Research Fund of the American Chemical Society, through Grant #PRF 1633-A3, is gratefully acknowledged.

## NOTATION

- $a_n (n = 0, 1, 2 \dots) =$  coefficients in expansion Equations (39), (42)
- $c =$  gas concentration in the interparticle space, mole/ml.
- $c_i =$  gas concentration inside the particle, mole/ml.
- $c_{ads} =$  surface concentration expressed as amount adsorbed per unit weight of adsorbent, mole/g. sorbent
- $c_s =$  surface concentration, amount adsorbed per unit area of the adsorbent surface, mole/sq.cm.
- $c_{s,p}, c_{s,ps}, c_{s,s} =$  surface concentration, amount adsorbed per unit of volume of pores, of particle, of solid, respectively, mole/ml.
- $D_c =$  effective intraparticle diffusion coefficient, Equation (7), sq.cm./sec.
- $D_K =$  effective gas (Knudsen) diffusion coefficient, sq.cm./sec.
- $\mathcal{D}_K =$  Knudsen diffusivity, sq.cm./sec.
- $\mathcal{D}_s =$  true surface diffusion coefficient, [Equation (1)], sq.cm./sec.
- $\mathcal{D}_{AB} =$  binary gas diffusion coefficient, sq.cm./sec.
- $D_{s,p}, D_{s,ps}, D_{s,s} =$  effective surface diffusion coefficients, Equation (3), sq.cm./sec.
- $E_A =$  effective axial dispersion coefficient, sq.cm./sec.
- $\Delta H_{ads} =$  heat of adsorption, kcal./mole
- $h(p) =$  function defined by Equation (17)
- $H_n(\tau) =$  Hermitian polynomial, Equation (40)
- $K_A =$  adsorption equilibrium constant (adsorption coefficient), ml./g.
- $k_f =$  mass transfer coefficient, Equation (12), cm/sec.
- $m_n =$  integral, Equation (20)
- $M =$  molecular weight, g./mole
- $N_{s,A}^* =$  surface flux, Equation (1), mole/sec.cm.
- $N_s =$  surface flux, Equation (3), mole/sec.sq.cm.
- $N_{NuAB} =$  Sherwood number,  $2R k_f / \mathcal{D}_{AB}$
- $p =$  variable in the Laplace-Carson transformation
- $q_{ext} =$  tortuosity factor for axial dispersion, Equation (38)
- $q_{int} =$  tortuosity factor for intraparticle gas diffusion, Equation (10)
- $q_{surf} =$  tortuosity factor for intraparticle surface transport, Equation (9)
- $R =$  radius of the spherical particle, cm.
- $R_g =$  gas constant
- $\bar{r} =$  average pore radius, cm.
- $r =$  radial coordinate in the spherical particle
- $s(z,p) =$  Laplace-Carson transform of  $c(z,t)$ , Equation (15)
- $t =$  time, sec.
- $t_{oA}, (t_o)_{inert} =$  injection time for adsorbable or unadsorbable substance, sec.
- $v =$  carrier gas velocity in the interparticle space, cm./sec.
- $w(t) =$  deflection of the recorder pen
- $x =$  coordinate in the direction of the surface flux
- $z =$  coordinate along the length of the chromatographic column

## Greek Letters

- $\alpha$  = external void fraction  
 $\beta$  = intraparticle void fraction  
 $\gamma$  = function defined by Equation (16)  
 $\delta_o, \delta_1, \delta_2, \delta_e, \delta_i$  = groups of constants defined by Equations (26), (27), (28), (36), and (37)  
 $\lambda$  = expression defined by Equation (18)  
 $\mu'_n, \mu_n$  =  $n$ th absolute and central moment, respectively, Equations (19), (21)  
 $\tau$  = reduced time defined by Equation (41)  
 $\theta_{\text{propane}}$  = coverage of the adsorbent surface, fraction of a monolayer

## LITERATURE CITED

- Schneider, P. and J. M. Smith, *AIChE J.*, **14**, 762 (1968).
- Kubin, M., *Collection Czech. Chem. Commun.*, **30**, 1104 (1965).
- Ibid.*, 2900.
- Haul, R. A. W., *Angew. Chem.*, **62**, 10 (1950).
- Gilliland, E. R., R. F. Baddour, and J. L. Russell, *AIChE J.*, **4**, 90 (1958).
- Carman, P. S., and F. A. Raal, *Proc. Roy. Soc. (London)*, **209A**, 38 (1951).
- , *Trans. Faraday Soc.*, **50**, 842 (1954).
- Carman, P. S., "Flow of Gases through Porous Media," Butterworth, London (1956).
- Ross, J. W., and R. J. Good, *J. Phys. Chem.*, **60**, 1167 (1956).
- Weaver, J. A., and A. B. Metzner, *AIChE J.*, **12**, 655 (1966).
- Masamune, S., and J. M. Smith, *ibid.*, **11**, 41 (1965).
- Eberly, P. E., and E. H. Spencer, *Trans. Faraday Soc.*, **57**, 284 (1961).
- Rossini, F. D., K. S. Pitzer, R. L. Arnett, R. M. Braun, and G. C. Pimentel, "Selected Values of Physical and Thermodynamic Properties of Hydrocarbons and Related Compounds," Carnegie Press, Pittsburgh, Pa. (1953).
- Haul, R. A. W., *Z. physik. Chem.*, **1**, 153 (1954).
- Barrer, R. M., and T. Gabor, *Proc. Roy. Soc. (London)*, **256A**, 267 (1960).
- Bird, R. B., W. E. Stewart, and E. N. Lightfoot, "Transport Phenomena," John Wiley, New York (1960).
- Reid, R. C., and T. K. Sherwood, "The Properties of Gases and Liquids," McGraw-Hill, New York, (1958).
- Kuvera, E., *J. Chromatography*, **19**, 237 (1965).
- Taylor, G. L., and J. H. Atkins, *J. Phys. Chem.*, **70**, 1051 (1966).
- Gorring, R. L., and A. J. deRosset, *J. Catalysis*, **3**, 341 (1964).
- Weisz, P. B., and A. B. Schwartz, *ibid.*, **1**, 399 (1962).
- Satterfield, C. N., and T. K. Sherwood, "The Role of Diffusion in Catalysis," Addison-Wesley, Reading, Mass. (1963).
- Barrer, R. M., and J. A. Barrie, *Proc. Roy. Soc. (London)*, **213A**, 250 (1952).
- Smith, R. K., and A. B. Metzner, *J. Phys. Chem.*, **68**, 2741 (1964).
- Gelbin, D., *Chem. Techn.*, **18**, 200 (1966).
- Barrer, R. M., *J. Phys. Chem.*, **57**, 35 (1953).

Manuscript received July 6, 1967; revision received November 9, 1967; paper accepted November 30, 1967.

# Two Phase Friction Factor for Para-Hydrogen between One Atmosphere and the Critical Pressure

JOHN D. ROGERS

Los Alamos Scientific Laboratory, University of California, Los Alamos, New Mexico

The Martinelli model for pressure drop in flowing two-phase systems has been examined in detail for para-hydrogen from 1 atm. to its critical pressure. A method for obtaining the Martinelli  $\Phi$  term, two phase friction factor, at intermediate pressures is presented.  $\Phi^2$  can be expressed as a function of pressure and quality. The Martinelli  $\beta$  term, ratio of actual vapor or gas area to an idealized cylindrical area, is found to vary greatly and to indicate first an increase in gas-liquid interface to gas volume ratio and then a decrease with increasing pressure. Some experimental data are examined in light of this development.

A need exists for a semi-empirical, theoretical method to predict pressure drop for flowing two phase systems at pressures other than those for which data is readily obtained. Most often for one component systems, data are limited to near atmospheric conditions or at best to a few pressures intermediate between one atmosphere and the critical condition. This development offers a means of determining the two phase pressure drop for one component systems over the entire regime of gas-liquid coexistence,

provided a good estimate can be made of either  $\alpha$  or  $\beta$  as defined for the Martinelli, et al. model (1). This development has been performed for para-hydrogen.

## $\Phi$ VS. $X$ AT INTERMEDIATE PRESSURES

Figure 1 gives the  $\Phi$ ,  $R_i$ ,  $X$  relationships as presented by Lockhart and Martinelli (2). Only  $\Phi$  for the liquid, turbulent-turbulent system will be considered; hence no subscripts will be carried on  $\Phi$  or other terms if not needed.